E3-2004-216

A. I. Frank[1], S. N. Balashov[2,3], I. V. Bondarenko[1],
P. Geltenbort[4], P. Hoghoj[4,5], A. V. Kozlov[1,6],
S. V. Masalovich[2,9], B. P. Toperverg[7,8]

RESONANT TUNNELING OF UCN THROUGH THE MOVING INTERFERENCE FILTER AND EXPERIMENTAL TEST OF THE UCN DISPERSION LAW

[1]Joint Institute for Nuclear Research, Dubna
[2]RRC Kurchatov Institute, Moscow
[3]University of Sussex, UK
[4]Institute Laue–Langevin, Grenoble, France
[5]XENOX, Grenoble, France
[6]Weissmann Institute of Physical Sciences, Israel
[7]Research Centre Juelich, Germany
[8]PNPI, Gatchina, Russia
[9]TU Muenchen, Germany

Франк А. И. и др. Е3-2004-216
Резонансное туннелирование УХН сквозь движущийся интерференционный фильтр и экспериментальная проверка закона дисперсии для УХН

Для проверки справедливости закона дисперсии очень медленных нейтронов нами был исследован спектр ультрахолодных нейтронов (УХН) в условиях резонансного туннелирования сквозь движущийся нейтронный интерференционный фильтр. Спектр характеризуется узкой резонансной линией, параметры которой зависят от характеристик фильтра и закона дисперсии нейтронной волны. Для ряда образцов был обнаружен заметный сдвиг положения резонанса при движении фильтра параллельно своей поверхности, что сильно противоречит общепринятому закону дисперсии. Дальнейшие исследования показали, что спектр протуннелировавших нейтронов не определяется строгим решением одномерной квантовой проблемы, а существенно искажается эффектом рассеяния нейтронов на неоднородностях фильтра. Сечение этого рассеяния зависит от волнового числа нейтрона и очень сильно возрастает в условиях резонанса. Экспериментальные результаты и проведенный нами теоретический анализ позволяют заключить, что наиболее вероятной причиной обнаруженного явления сдвига резонанса в движущемся образце является рассеяние нейтронов в условиях резонансного туннелирования, а не отклонение от общепринятого закона дисперсии.

Работа выполнена в Лаборатории нейтронной физики им. И. М. Франка ОИЯИ и Институте Лауэ–Ланжевена, Франция.

Сообщение Объединенного института ядерных исследований. Дубна, 2004

Перевод авторов

Frank A. I. et al. E3-2004-216
Resonant Tunneling of UCN through the Moving Interference Filter and Experimental Test of the UCN Dispersion Law

With the aim to test experimentally the dispersion law validity for very slow neutrons we investigated spectra of ultracold neutrons (UCN) under the condition of resonance tunneling through the moving Neutron Interference Filters. The neutron spectrum in this case has a narrow width resonance, whose parameters depend on the filter characteristics and dispersion law of neutron waves in matter. For a number of samples we detected noticeable shift of the resonance position when filter moved parallel to its surface. This shift is in strong contradiction with the commonly accepted dispersion law. Further investigations have shown that spectrum of tunneling neutrons is not exactly defined by the solution of one-dimensional quantum problem, but substantially affected by neutron scattering from filter imperfections. The cross section of this scattering depends on the neutron wave number and increases dramatically in resonance conditions. Experimental results as well as comprehensive theoretical analysis have led us to the unambiguous conclusion that observed phenomena of the resonance shift in a moving sample are caused by scattering of neutron tunneling states rather than by a deviation from the commonly accepted dispersion law.

The investigation has been performed at the Frank Laboratory of Neutron Physics, JINR, and Institute Laue–Langevin, France.

Communication of the Joint Institute for Nuclear Research. Dubna, 2004

INTRODUCTION

A neutron interference filter (IF) is an analog of an optical Fabry–Perot interferometer. In the simplest case, it represents a three-layer thin-film structure of two different materials deposited onto a substrate transparent to neutrons. Neutron refraction at the interfaces between layers is described with the use of an effective potential U associated with each material:

$$U = \frac{2\pi\hbar^2}{m}\rho b. \tag{1}$$

Here ρ is the number of nuclei per unit volume, b is the coherent scattering length, and m is the neutron mass. Materials for the filter are chosen in such a way that the effective potential of the exterior layers is higher than that of the interior layer. Therefore the potential structure of the filter represents two barriers and a well in between. If the thickness of the interior layer is not overly small,

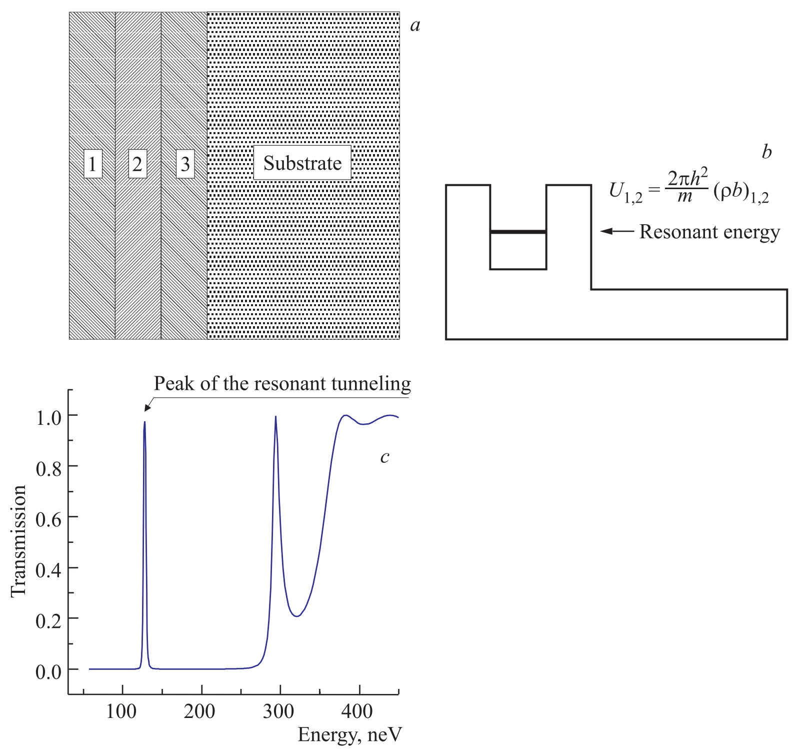

Fig. 1. Neutron interference filter. Three thin films of two kinds of materials deposed at a silicon wafer (*a*). Potential structure of the system (*b*). Transmittivity of filter as a function of energy (*c*)

the quasi-bound states appear with characteristic energy levels. In the vicinity of these levels, neutron transmission features the resonance structure (see Fig. 1).

The position of the resonance is determined by the matching of the wave functions at the layer boundaries, whereas its width depends on the penetrability of the exterior layers. According to the commonly accepted dispersion law, all features in the transmission of an ideal filter are determined entirely by the normal components of real- or imaginary-valued wave vectors.

The possibility to produce a two-humped potential structure for implementing a resonance transmission of ultracold neutrons (UCN) was indicated in 1977 by Seregin [1]. Later on it was proposed to use such interference filters as a very sensitive device for the measurement of a small energy or momentum transfer utilizing UCN [2]. In 1980, the resonance tunneling of UCN through the three-layer Cu–Al–Cu filter was demonstrated experimentally by A. Steyerl with co-authors [3] and later by M. Novopoltsev and Yu. Pokotilovsky [4, 5]. The effect of resonance splitting in a system of two coupled resonators was also demonstrated in an experiment with five-layer IF [6, 7]. Frank and Nosov proposed to use a spectrometer with IF in order to detect the discrete spectrum of UCN that arises as a result of diffraction by a grating, which moves in the direction transverse to the incident neutron beam [8, 9]. Somewhat later, it was proposed to use a similar device in order to test the commonly accepted dispersion law for UCN in medium [10]. This and some other possibilities were analyzed in [11].

In 1997, the UCN spectrometer with IF was built up [12] and experimental test of the UCN dispersion law started. First results were reported in [13]. Description of the spectrometer, results of the further investigations and new proposals were published in [14–17]. The same device was used in the experiment on neutron diffraction by a moving grating [18, 19], which was proposed in [8, 9].

In the process of the work, it was recognized that spectrum of UCN after tunneling through the filter differs, sometimes remarkably, from the spectrum predicted by the elementary theory. In this paper, we investigate this phenomenon and its influence on the test of the dispersion law validity.

1. NEUTRON TRANSMISSION THROUGH THE MOVING INTERFERENCE FILTER AND EXPERIMENTAL TEST OF THE UCN DISPERSION LAW

1.1. The Idea of the Experiment. In this section, we describe briefly the experiment for testing the UCN dispersion law. It is well known that the dispersion law for the neutron wave in medium may be written as [20]

$$\mathbf{k}^2 = \mathbf{k}_0^2 - \chi_0^2, \quad \chi_0^2 = 4\pi\rho b, \quad b = b' - ib'', \tag{2}$$

where $\mathbf{k}_0$ and $\mathbf{k}$ are neutron wave vectors in vacuum and in medium respectively. The effective potential (1) corresponds just to this relation. It is commonly accepted that precision of Eq. (2) in case of very cold neutrons is very high and rises as wave length increases [21–23]. However some theoretical arguments put in doubt the correction of this concept [10, 24]. Below we present experimental results, which could establish the extent to which the relations (1), (2) are valid in UCN physics.

The idea of the experiment is based on the specific properties of the potential dispersion law [25, 26]. Let us consider a neutron wave refracted at the boundary of medium and suppose that the dispersion law differs from Eq. (2) by an additional term $\varepsilon(\mathbf{k}_0^2)$:

$$\mathbf{k}^2 = \mathbf{k}_0^2 - \chi_0^2 + \varepsilon(\mathbf{k}_0^2). \tag{3}$$

For a homogeneous medium the wave vector component $\mathbf{k}_{0,t}$, parallel to the plane of the interface, does not change by refraction. Subtracting $\mathbf{k}_t^2 = \mathbf{k}_{0,t}^2$ from both sides of Eq. (3) we obtain

$$\mathbf{k}_\perp^2 = \mathbf{k}_{0\perp}^2 - \chi_0^2 + \varepsilon(\mathbf{k}_0^2). \tag{4}$$

One may conclude that the existence of the nonpotential term $\varepsilon(\mathbf{k}_0^2)$ causes the normal component of the wave vector in medium $\mathbf{k}_\perp$ to depend on the value of the wave vector in vacuum $\mathbf{k}_0$. The goal of the presented experiment is a search for this dependence with utilizing a neutron interference filter as a high sensitive device.

Let us consider a filter moving parallel to its surface. In the frame of reference of this filter, the lateral component $\mathbf{k}_{0,t}$ of the incident wave as well as the total vector $\mathbf{k}_0$ are changed. Obviously the normal component $\mathbf{k}_{0,t}$ of the wave vector of the incident wave does not depend on the movement. However, in the case of nonpotential dispersion law the normal component of the wave vector $\mathbf{k}_\perp$ inside the medium depends on the movement and changes according to Eq. (4). This consequently leads to a shift of the resonance position. This shift can be detected with a high-precision UCN spectrometer described below.

1.2. Experimental Set-up. Gravity Spectrometer with Interference Filters. We have constructed a special spectrometer dedicated to the experimental test of the UCN dispersion law [13–14] (see Fig. 2). Main elements of the spectrometer are two different IFs, each having only one resonance in transmission. They are placed horizontally at different heights, one above the other, inside a hexagonal neutron mirror guide with vertical glass walls. Neutron spectrum after the upper filter (monochromator) is defined by the resonance in transmission of this filter and varies with height as neutrons fall in a gravity field. The lower filter (analyser) features the resonance at a higher neutron energy compared to the upper filter. So the total transmission of two filters depends on the distance between them. Changing the height of the filter-analyser and measuring a count rate as a function of the distance between the filters, one may scan the energy spectrum of neutrons passed through the upper filter-monochromator. Both filter-monochromator and filter-analyser feature the relatively narrow resonance with a width of about 4 neV.

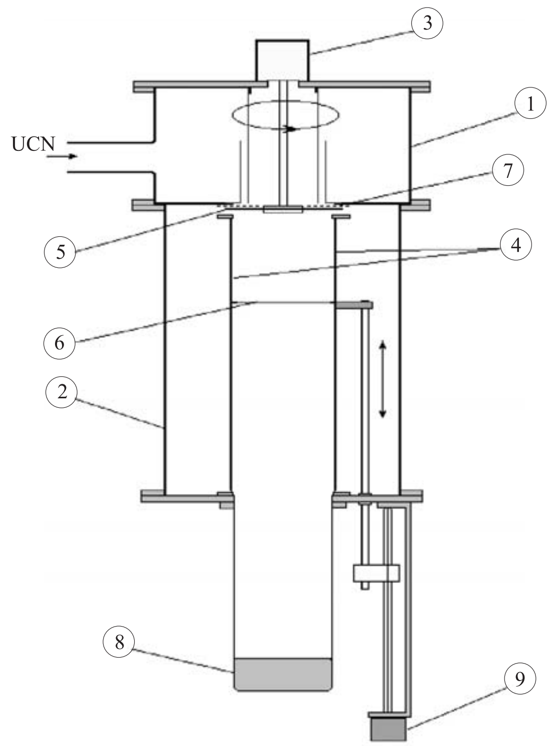

Fig. 2. Gravity UCN spectrometer with interference filters. 1 is an entrance chamber; 2 is a vacuum vessel; 3 is a high-speed motor; 4 is a mirror neutron guide; 5 is a filter-monochromator (movable); 6 is a filter-analyser; 7 is a removable filter (premonochromator in special experiments); 8 is a detector; 9 is a stepper motor

UCNs enter the spectrometer from the source and after several reflections off the walls of the entrance chamber pass through the cylindrical corridor. The corridor guides the neutrons to the filter-monochromator and enables the UCNs to irradiate only the peripheral area of the silicon disk with a deposited filter on it. The disk is attached to the motor shaft and may rotate around the vertical axis that causes the lateral component $\mathbf{k}_{0,t}$ of the incident wave to vary in the frame of reference of the filter. A precise stepper motor is used to change the vertical position of the filter-analyser. Neutrons passed through this filter are counted with a ^{3}He proportional detector.

1.3. Experimental Procedure and Main Results. The experiment was performed at the UCN source of the ILL [27]. To test the validity of Eq. (2), the scanning curve mentioned above was measured twice: with the filter-monochromator at rest (or spinning very slowly) and with fast spinning filter. The result of scan-

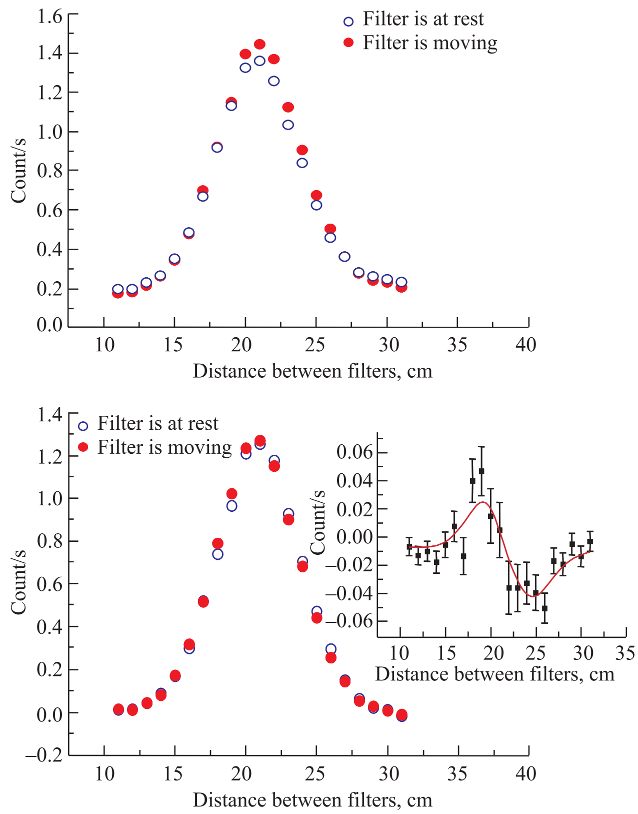

Fig. 3. Scanning curves obtained in 1998. The error bars are smaller than the point size. Raw data are presented at the top. The same resuls after normalizing and subtracting the background are at the bottom. The insert shows the behaviour of the difference between two normalized scanning curves

ning is the convolution of the spectrum $f(E)$ after the filter-monochromator and the spectral function of the filter-analyser $g(E)$:

$$F(z) = \int f(E)g(E-z)dE, \quad (5)$$

where $z = mg\Delta H$ and ΔH is the distance between the filters. Taking into account that $g(E)$ does not depend on the rotation of the filter-monochromator, one may conclude that any changes in scanning curve $F(z)$ may result only from the variation of the spectrum $f(E)$.

During the first experiments in 1997 [13, 14], it has been found that spectrum of neutrons, passed through the filter-monochromator, varies when filter is put in rotation. These variations are the following: a) a peak area decreases; b) a count rate outside the peak increases slightly, which may be interpreted as increase of the background; c) a noticeable shift of the peak is observed when filter is spinning. One may see all these variations in Fig. 3, where two scanning curves with and without filter rotation are presented. The rotation frequency was 5400 rpm and linear velocity of the filter rim was about 36 m/s. The peak shift was measured to be $\Delta E = +0.098 \pm 0.016$ neV.

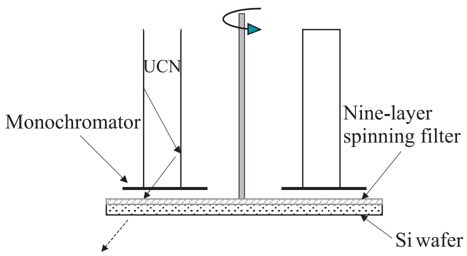

Fig. 4. Lay-out of the test experiment

We performed this experiment again in 1998 [15, 16] both with old and new filters. Some filters were made of new materials. The results obtained during this run are in good agreement with the previous ones. Our investigations showed that neither statistical fluctuations nor any trivial parasitic effects [15, 16] could explain the peak shift observed in these measurements.

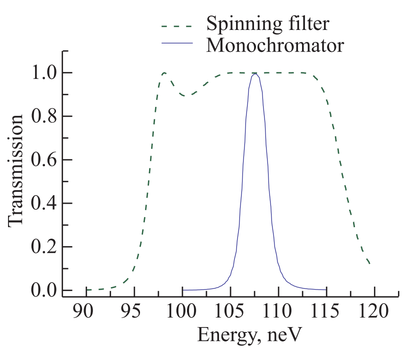

Fig. 5. Calculated transmittivity of the filters in test experiment

We describe here one of the test experiments. The aim was to exclude from consideration the hypothesis that observed changes in the neutron spectrum are due to interaction of neutron waves with different imperfections of a rotating disk like macroscopic waviness or wedge shaping. In this experiment we used filter-monochromator fixed at the exit of annular corridor (see Fig. 4). Neutrons with relatively narrow spectrum after this filter irradiate another filter with wide transmission peak (Fig. 5). This second filter is located just below the first one and may be put in rotation with a motor. The experimental procedure and data processing were the same as in the main experiment. No change in the peak position under filter spinning was observed: $\Delta E = +0.009 \pm 0.024$ neV.

Nevertheless in 1999 we designed new filters utilizing Ni(N)–Ti/Zr layers. For these filters we did not observed any shift of the transmission peak position when we changed frequency of filter rotation from 3 Hz to 90 Hz. The obtained result [15, 16] was in a dramatic contradiction with the previous one. Another distinctive feature of these filters is a much less decrease of a peak area under rotation (less than 3%), which indicates the better quality of interfaces. The summary of the results are presented in table below.

Measured shift of the resonance position under variation of initial wave vector from $k_0 \cong 8.5 \cdot 10^5$ cm^{-1} to $k_0 \cong 5 \cdot 10^6$ cm^{-1}

	Date	Filter-monochromator		ΔE, neV	Peak area decrease, %
		Number	Type		
1	1997	1	Ni(N)–Ti/Zr	$+0.098 \pm 0.016$	
2	1998	1	Ni(N)–Ti/Zr	$+0.093 \pm 0.024$	10
3	1998	1	Ni(N)–Ti/Zr (Improved experimental conditions)	$+0.075 \pm 0.019$	
4	1998	2	Ni(N)–Ti splitted	$+0.180 \pm 0.045$	40
5	1998	3	Ni(N)–Ti	$+0.202 \pm 0.085$	40
6	1998	4	Ni(N)–Ti/Zr (nine layers)	$+0.040 \pm 0.014$	6
7	1999	5	NiV(7%)–Ti	$+0.084 \pm 0.017$	17
8	1999	6	Ni(N)–Ti/Zr splitted	-0.060 ± 0.082	< 3
9	1999	7	Ni(N)–Ti/Zr	$+0.001 \pm 0.007$	< 3

For most of the measurements, we used five-layer filters with three-barrier potential structure. Such quasi-symmetrical structure is characterized by the splitting of the resonance levels. The value of this splitting is defined by a width of the central barrier located between the wells. For filters 1–3, 5, and 7 (see table), such splitting is less than the width of the resonance and two states degenerate. For filters 2–6, two resonance levels are resolved clearly [14, 17]. Filter 4 is a nine-layer filter with a relatively wide resonance.

So we may summarize our results as follows: 1) for a number of filters we observed the transformation of the transmitted spectrum under rotation; 2) this transformation has a complicated character and includes a shift of the peak position; 3) this phenomenon is not universal and depends on the filter properties. To explain these results, one may suppose that the origin of this transformation is neutron scattering at internal imperfections of filter. Obviously such scattering depends on the value of the wave vector and thus may vary when filter rotates.

2. FILTER IMPERFECTIONS AND MODIFICATION OF THE TRANSMITTED NEUTRON SPECTRUM

2.1. Neutron Scattering by Roughness at Resonance Tunneling. It is obvious that materials of a real filter are not absolutely homogeneous and interfaces between layers are not ideally flat and smooth. In both cases the deviation from the ideal structure may be described via introduction of perturbation potential $\Delta U(r)$, which results in scattering. The latter occurs in addition to the transmission through, reflection from, and refraction in the mean optical potential $U(z) = \langle \Delta U(r) \rangle$ averaged over lateral directions. This part of the interaction potential is a function of the only coordinate z normal to the sample surface. If the scattering effect is weak then corrections to the exact wave function found for the main potential $U(z)$ can be accounted for within the framework of the perturbation theory approach, i.e. of the Distorted Wave Born Approximation (DWBA) [28–32]. Scattering cross section and scattering amplitude in DWBA are then defined as

$$\frac{d\sigma}{d\Omega} = |f(\mathbf{k}_f, \mathbf{k})|^2, \quad f(\mathbf{k}_f, \mathbf{k}) = -\frac{m}{2\pi\hbar^2} \int dr \Psi_i(\mathbf{r}, \mathbf{k}) \Delta U(r) \tilde{\Psi}_f(\mathbf{r}, \mathbf{k}_f), \quad (6)$$

where $\Psi_i(\mathbf{r}, \mathbf{k}) = \psi(\mathbf{z}, \mathbf{p}_i) \exp(\mathbf{i}, \kappa_i \rho)$ and $\tilde{\Psi}_f(\mathbf{r}, \mathbf{k}_f) = \tilde{\psi}(\mathbf{z}, \mathbf{p}_f) \exp(-\mathbf{i}, \kappa_i \rho)$ are exact solutions for the same potential $U(z)$, but with different asymptotic conditions: $\Psi_i(\mathbf{r}, \mathbf{k})$ is the wave function of neutrons, which are free before interaction with the potential and impinging onto the sample surface with the wave vector $\mathbf{k} = \{\kappa_i, \mathbf{p}_i\}$, while $\tilde{\Psi}_f(\mathbf{r}, \mathbf{k}_f)$ corresponds to the propagation of neutrons asymptotically free at infinity and falling onto the sample with wave vector $\mathbf{k}_f = \{-\kappa_i, -\mathbf{p}_f\}$ reversed with respect to that of scattered from the sample [31] (see Fig. 6). Here $\mathbf{p}_f = \mathbf{k}_f \sin(\Theta_f)$, and $\mathbf{p}_f = -\mathbf{k}_f \sin(\Theta_f)$ are transverse, while κ_i and κ_f are lateral components of the incoming and outgoing wave vectors, respectively; Θ_i is the glancing angle of incidence and Θ_f is the glancing angle of scattering, $\hbar^2 \mathbf{k}_i^2 = 2mE_i$, $\hbar^2 \mathbf{k}_f^2 = 2mE_f$, E_i and E_f are energy of incident and, respectively, final neutron state. At elastic scattering $E_i = E_f$.

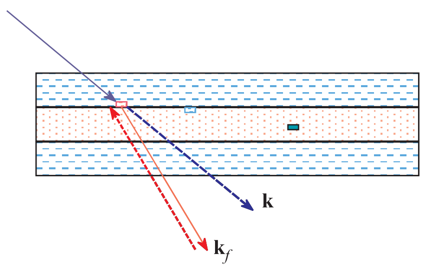

Fig. 6. Scattering by roughness

Substitution of the explicit form wave function allows one to rewrite the scattering cross section via the Fourier transform of the correlator $\langle \Delta U(\mathbf{r}) \Delta U(\mathbf{r}') \rangle$ of the scattering potential fluctuations:

$$\frac{d\sigma}{d\Omega} = \left(\frac{m}{2\pi\hbar^2}\right)^2 \int d\mathbf{r} d\mathbf{r}' \, e^{iq(\rho-\rho')} \psi(z, \mathbf{p}_i) \psi^*(z', \mathbf{p}_i) \times$$
$$\times \langle \Delta U(\mathbf{r}) \Delta U(\mathbf{r}') \rangle \psi(z, \mathbf{p}_f) \psi^*(z', \mathbf{p}_f), \quad (7)$$

where ρ and ρ' are the lateral coordinates, $\mathbf{q} = \rho - \rho'$ is the lateral momentum transfer.

It is easy to see that modulus of the scattering amplitude $|f(\mathbf{p}_i, \mathbf{p}_f)|$ increases dramatically when both incident and scattered wave vectors satisfy (or almost satisfy) condition for the resonance tunneling. If the initial wave function is normalized to unity, i.e. $|\Psi_i(0, \mathbf{k})|^2 = 1$ at the filter surface, then corresponding gain factor reaches a value of the order of $|\Psi(z, \mathbf{k}_r)|^2$ at a certain distance z where a scattering object (imperfection) is located. For a fife-layer filter this gain factor may reach 100 (see Fig. 7). As a scattering cross section is proportional to amplitude squared, so one may expect the scattering to become very strong at the resonance.

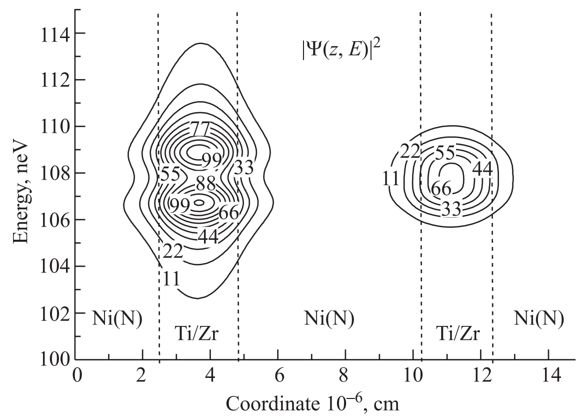

Fig. 7. Calculated $|\Psi|^2(z, E)$ inside a five-layer interference filter. Resonance splitting is of the order of the width of the resonance

Indeed our calculations based on the DWBA show the unlikely large value of the cross section in the close vicinity of the resonance conditions. This means that the DWBA, being a specific version of the perturbation theory, is not applicable within this range, where one should take into account modification of the wave functions in Eq. (6) due to scattering, i.e. solve the problem self-consistently. This would result in an effective additional broadening of the resonance lines due to the loss of intensity scattered from the well into the solid angle. If the total scattering cross section is, however, small with respect to the loss of intensity due to the finite width of the walls, then scattering contribution to the total broadening can be neglected. Otherwise, one may hope that DWBA describes the problem qualitatively.

The results of DWBA calculation under the assumption of uncorrelated roughness are as follows:

a) The scattering cross section is very large when both initial and final normal components of the $\mathbf{k}$ vector $\mathbf{p}_i$, $\mathbf{p}_f$ are close to the resonance value $\mathbf{k}_r$. The waves thus scattered may propagate either to the down hemisphere (transmission) or to the upper one (nonspecular reflection) resulting in a decreasing of a peak area.

b) The peak area also decreases due to scattering to the region out of the resonance. This decreasing is partly compensated by inverse process — scattering into the peak from far out-of-resonance regions. This process is also accompanied by off-specular scattering.

c) Calculations did not indicate any shift of the transmitted neutron spectrum.

d) When lateral component of the initial $\mathbf{k}$ vector increases due to filter moving, the scattering cross section decreases very fast.

Taking this into account, one may conclude that rotation is able to influence the intensity of the tunneled neutrons, but it causes its increase in apparent contradiction with experimental results. This discouraging conclusion is based on the results of traditional form of DWBA valid only for the case of purely elastic scattering, i.e. from a potential independent of time. This is certainly not the case for moving inhomogeneities, which implies explicit dependence of the potential $\Delta U(\mathbf{r}, t)$ on t.

Then one should develop perturbation theory for the solution of nonstationary Schrödinger equation with time-dependent perturbation. This can easily be done within the DWBA applicability range. Indeed, taking into consideration that the mean potential $U(z)$ is independent of time, one can use the same exact reference wave functions as found from the stationary Schrödinger equation $\Psi_i(\mathbf{r}, \mathbf{k}, t) = \Psi_i(\mathbf{r}, \mathbf{k}r)\, \mathrm{e}^{i\varepsilon_i t}$ and $\tilde{\Psi}_f(\mathbf{r}, \mathbf{k}_f, t) = \tilde{\Psi}_f(\mathbf{r}, \mathbf{k}_f)\, \mathrm{e}^{i\varepsilon_f t}$, modified with oscillating in time exponents, and write down the equation for double differential cross section as follows [32]:

$$\frac{d^2\sigma}{d\Omega d\omega} = \frac{m^2}{8\pi^2\hbar^5} \int d\mathbf{r}d\mathbf{r}'dt\, \mathrm{e}^{i\omega t}\Psi_i(\mathbf{r}, \mathbf{k})\Psi_i^*(\mathbf{r}', \mathbf{k})\times \\ \times \langle \Delta U(\mathbf{r}, t)\Delta U(\mathbf{r}', 0)\rangle \tilde{\Psi}_f^*(\mathbf{r}', \mathbf{k}')\tilde{\Psi}_f(\mathbf{r}, \mathbf{k}'), \quad (8)$$

where $\hbar\varepsilon_i = E_i$, $\hbar\varepsilon_f = E_f$ and $\hbar\omega = E_f - E_i$ is the energy transfer. Taking into account that at moving with the velocity vector $\mathbf{V}$ the correlator $\langle \Delta U(\mathbf{r}, t)\Delta U(\mathbf{r}', 0)\rangle = \langle \Delta U(\mathbf{r} - \mathbf{V}t)\Delta U(\mathbf{r}')\rangle$ and Eq. (8), one immediately finds that

$$\frac{d^2\sigma}{d\Omega d\omega} = \frac{d\sigma}{d\Omega} = \delta(\omega - \mathbf{qv}/\hbar). \quad (9)$$

Here it is very important to note that $\mathbf{q} = \mathbf{k}_f(\varepsilon_f) - \mathbf{k}_i(\varepsilon_i)$ and the equation $\hbar\omega = \mathbf{qv}$ have solutions depending on angles of incidence and scattering as well as on the velocity $\mathbf{V}$. At certain values of those parameters it may have no solution at all.

Later we consider the model that can explain observed results but now we present experimental data that revealed the distinguishing features of the resonance scattering.

2.2. Neutron Resonance Scattering and Mode Mixing. According to Eq. (6) the gain in scattering may take place not only for the small angle scattering when $\mathbf{k}$ vectors of initial and scattered waves are both close to the same resonance value $\mathbf{k}_r$ but also for a scattering when initial and scattered $\mathbf{k}$ vectors correspond to different resonances $\mathbf{k} \approx \mathbf{k}_r^{(i)} \rightarrow \mathbf{k}' \approx \mathbf{k}_r^{(j)}$, where $i, j = 1, 2$ is the number of resonance. To verify this statement, two interference filters, each having two resonances in the spectrum of transmitted neutrons, have been examined. These resonances are resolved clearly by the spectrometer. The modulus of undisturbed wave function inside each filter is presented in Fig. 8. Note that «energy» scale in Fig. 8 corresponds to the value $E_n = \dfrac{\hbar^2}{2m}\mathbf{k}_{0\perp}^2$ but not to the total energy. This means that transition between two different resonances in transmission may be caused by the scattering which does not change the total neutron momentum but only one of its components. We performed the measurements with two filters of different roughness to reveal clearly the effect of resonance scattering.

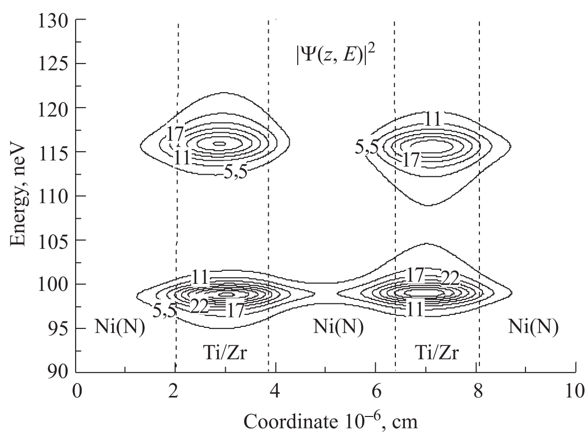

Fig. 8. Calculated $|\Psi^2|(z, E)$ inside a five-layer interference filter. Resonance splitting is greater than the widths of the resonance

The measurements were done at slow (3 Hz) and fast (90 Hz) rotations and with two different spectra of incident neutrons. One of them is the spectrum at the exit of the corridor while another one is modified by transmission of a thin film of Fomblin oil, deposited onto 10 μm aluminum foil (see Fig. 9) attached just below the corridor. In the last case, one may expect the intensity of the right peak on the scanning curve to be diminished significantly. At the same time the resonance scattering has the ability to reconstruct partly this peak, and the degree of this reconstruction depends on the neutron wavelength in the filter's frame of reference.

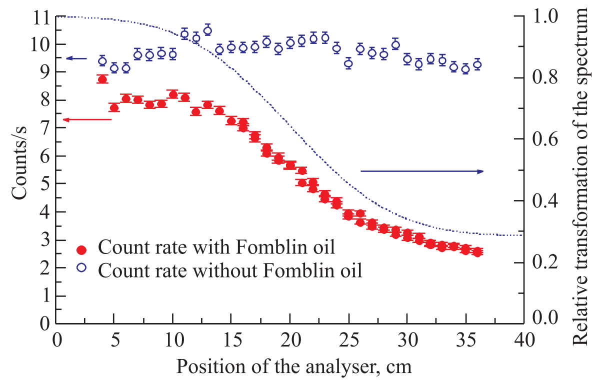

Fig. 9. Modification of the incident spectrum with Fomblin oil. Points represent count rate with and without spectrum filtering by «Fomblin». Dash line represents relative transformation of the spectrum

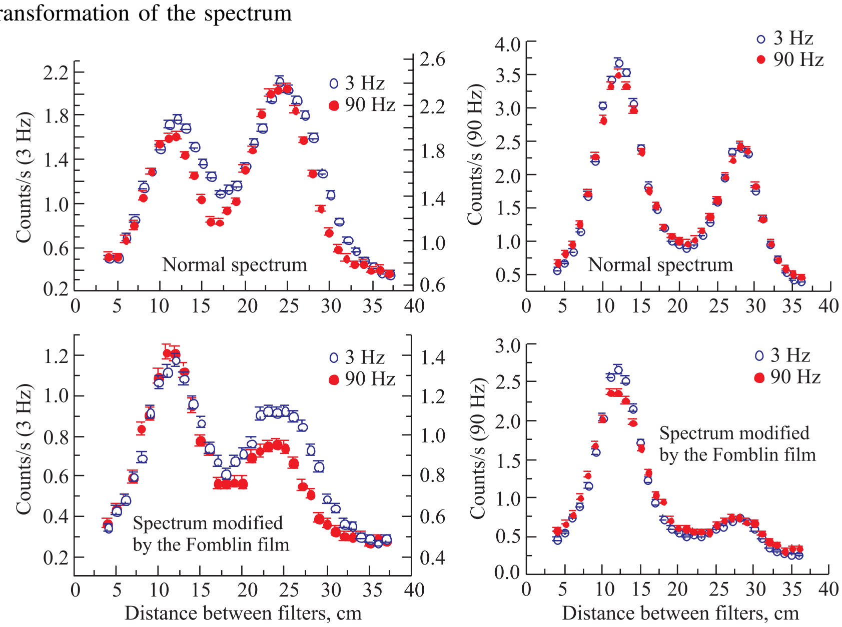

Fig. 10. Mode mixing due to resonance scattering

Figure 10 shows results of these measurements with two different filters. Data presented in the upper row correspond to the unmodified incident spectrum, and the lower ones, to the modified spectrum. One may easily see that filters feature very different properties. The intensity of neutrons, tunneled through the first filter (left column) decreases remarkably when filter rotates with a high frequency. This decreasing is about the same for both resonances. Notice that two different scales are used to plot the count rate for two spinning velocities. Besides, fast rotation is accompanied by the increasing of background. It is easy to see that the form of the transmitted spectrum depends on the rotation frequency. Under filter spinning both resonances get narrower and shift remarkably. With this filter all features of spectrum transformation may be seen by eye without any special data treatment. There is good reason to believe that this filter has magnetic inhomogeneities and these inhomogeneities increase in time. With modified spectrum we observed that the intensity of the right peak depends much more crucially on the rotation frequency than the intensity of the left peak.

So, the observed patterns are in good qualitative agreement with the assumption of partial reconstruction of spectrum due to resonance scattering. Indeed the rotation of filter causes an increase in the neutron wave vector in the filter's frame of reference and thus a decrease of the scattering cross section, which in turn diminishes the effect of spectrum reconstruction. At the same time for the filter with small inhomogeneities (Fig. 10, right column) the right resonance is suppressed significantly with modification of an incident spectrum and its intensity depends only slightly on the rotation frequency. From here on we will use the term «mode-mixing» for the resonance coupling effect observed in these experiments.

2.3. Neutron Scattering at Correlated Roughnesses. Here we continue to discuss our results obtained with filters that feature only one resonance in transmission. One may assume that detected decrease of a peak area and accompanied increase of the background result from the neutron scattering by moving roughnesses or inhomogeneities. At the same time the calculations of the scattering cross section in the first order of DWBA do not confirm this assumption. However it should be remembered that these calculations were made under assumption of noncorrelated scatters, whereas the joint action of correlated scatters may differ significantly from the action of a single scatter. Fast movement of an object with correlated scatters on/in it may lead to new effects in scattering which are not observed when the sample is at rest. Recently observed neutron diffraction by a moving grating [8, 18, 19] provides an example where a regular structure of a grating comprises a limiting case of correlated scatters.

Let us assume that a regular structure with a space period L is moving with a velocity V across the neutron beam along the positive direction of the y axis. Generally waves passed through the different areas of the grating differ in their intensities or/and phases. Thus the moving grating modulates the transmitted waves at each point of the beam cross section with the frequency $\Omega = 2\pi V/L$. The resulting spectrum of the transmitted waves will therefore be discrete and described by the following wave function:

$$\Psi(x,t) = \sum_{n=-\infty}^{\infty} a_n \exp\left[i(k_n x - \omega_n t)\right], \tag{10}$$

where $\omega_n = \omega + n\Omega$, and $k_n = k(1 + n(\Omega/\omega))^{1/2}$ for the case of $\Omega/\omega \ll 1$. The resulting frequencies ω_n correspond to the particle energies $E_n = \hbar(\omega + n\Omega)$, where $\hbar$ is the Planck constant. The intensities of partial waves are $I_n \left|a_n\right|^2$, where a_n are the Fourier coefficients of the modulation function.

In [8, 9], this result was obtained with the use of another and more rigorous approach. The diffraction problem has been solved by subsequent application of the Galilean transformation to the wave function. The result for the small diffraction angles is

$$\Psi(x, y, t) = \sum_n c_n \exp\left[i(k_n x + \alpha_n y - \omega_n t)\right], \tag{11}$$

where $\alpha_n = (2\pi/L)n$.

Equation (11) differs from Eq. (10) by the diffraction term $\alpha_n y$. Besides, Fourier coefficients c_n in (10) are obtained from the $k \leftrightarrow x$ Fourier transformation of the spatial variation of the transmitted wave amplitude, while coefficients a_n in (11) result from $\omega \leftrightarrow t$ Fourier transformation of temporal variation of the transmitted amplitude. Equation (11) transforms into Eq. (10) if the grating velocity V and grating space period L are both become large with the same modulation time $T = L/V$. Thus fast moving of grating across the neutron beam may be considered as temporal modulation of the transmitted neutron wave. As a consequence the set of coherent waves with the spectrum defined by the modulation function appears.

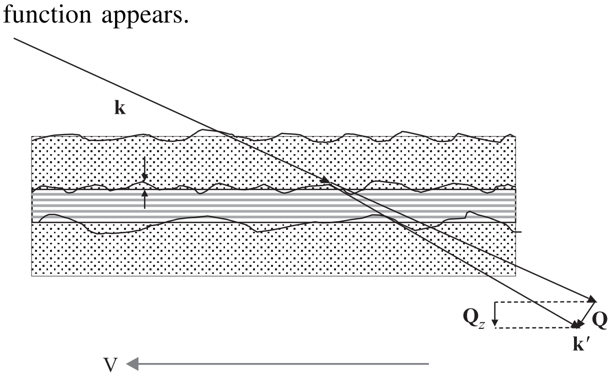

Fig. 11. Diffraction from the rough interfaces

Coming back to the case of the filter with correlated roughnesses, we can now predict qualitatively the result of its fast moving. Utilizing the main idea of the DWBA as a perturbation theory (see, for example, [30]), we may represent the filter as a combination of an ideal multilayer structure and aperiodic potential $\Delta U(y, z)$ caused by correlated roughness or waviness (see Fig. 11).

Zero-order solution for the wave function which describes neutron beam passed through an ideal multilayer structure may be found with any standard method. Due to ideality of the structure this solution is invariant with respect to the sample movement parallel to the filter surface. At the same time the potential $\Delta U(y, z)$ moving along y axis will modulate neutron waves acting as an aperiodic moving grating. For the transferred energy and momentum, in this case one may write

$$\Delta E \approx \hbar \frac{\pi v}{\ell}, \quad \Delta Q_z \approx \frac{2\pi}{\ell} \frac{V}{v_z}, \tag{12}$$

where ℓ is the correlation length of roughness or waviness, and v_z is the normal component of the neutron velocity.

It is worth noting that in case of resonance transmission even relatively small deviations from an ideal structure may result in a deep modulation of intensity and phase of the transmitted wave.

The model described above can explain our experimental results concerning the peak area and background changes. Indeed as the transferred momentum is relatively large so all «accelerated» neutrons may pass freely through the filter-analyser, which gives rise to the additional background. At the same time, as neutrons with resonance energy exhibit a much stronger scattering, the peak area decreases. In addition some neutrons may decrease their energy after passing through a rotating filter. Such «decelerated» neutrons are reflected by the analyser and finally are lost.

2.4. Forward Scattering and Interference Cross Section. Shift of the resonance position under filter rotation observed in our first measurements and lack of any shift in the last measurements is evidently the most intriguing result. As already noticed above, calculations in the first order of DWBA do not explain this effect. However situation changes dramatically if one takes into account the interference of the scattered wave with that part of the incident wave that passes through the filter without scattering. Such interference plays an important role providing the conservation law of the total flux [31].

Corresponding interference cross section is defined as

$$\sigma_{ti} = -\frac{4\pi}{k} \operatorname{Im} \{T^* f(\mathbf{k}, \mathbf{k})\}, \tag{13}$$

where T is the amplitude of transmission through the ideal filter and $f(\mathbf{k}, \mathbf{k})$ is given by Eq. (6) with $\mathbf{k} = k_f$. Both values T and f are complex functions. Figure 12 displays the behaviour of the interference cross section σ_{ti} in the region of resonance calculated for our filters. Notice that interference cross section changes its sign in the region of resonance. Taking into account that positive sign of the cross section corresponds to the destructive interference decreasing the transmitted flux, whereas negative sign corresponds to the constructive interference increasing the transmitted flux, one can conclude that the transmitted neutron spectrum will be effectively shifted to the low-energy region. It is worth to note that due to $1/k$ factor in (13) this interference effect becomes most important in the event of

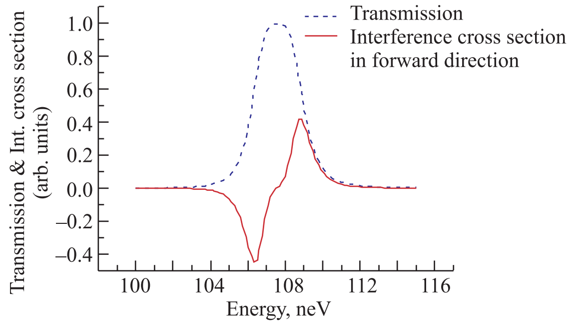

Fig. 12. Interference cross section for the forward scattering in the case of five-layer filter and spectrum of transmitted neutrons for the ideal filter (dashed line)

normal incident of neutrons onto a filter at rest. In this case, the line shape and position of the resonance obtained for a nonideal filter greatly differs from that obtained for the ideal one with the same set of parameters. Under rotation, when total **k** vector is large enough, the effect of interference becomes relatively small.

This means that filter rotation leads to the reconstruction of the spectrum typical for an ideal filter, which in turn leads to the shift of the resonance position to the high-energy region. It is precisely the result we observed in our experiments (see table).

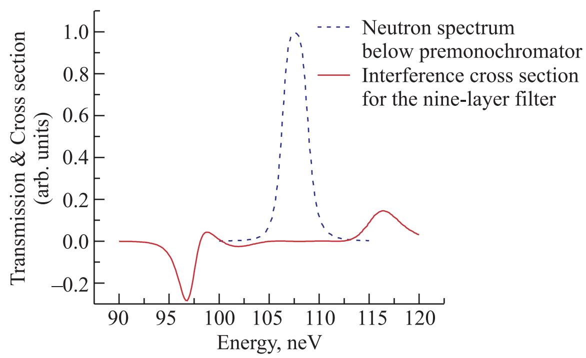

Fig. 13. Interference cross section for the forward scattering in the case of nine-layer filter used in the test experiment and spectrum, and spectrum of transmitted neutrons, which was formed by premonochromator (dashed line)

This model can be also applied to explain results obtained in the test experiment described in Sec. 1.3. The variation of spectrum in this special case was found to be relatively small since the interference cross section calculated for the broad-band spinning filter differs noticeably from zero only in regions where there are no neutrons passed through the filter-premonochromator (Fig. 13). So the forward scattering interference in the spinning filter has no effect on the final transmitted spectrum.

CONCLUSION

We may summarize that the spectrum of UCN passed through a nonideal interference filter differs from the solution for one-dimensional problem. Generally it is distorted and shifted due to scattering by roughness and filter's inhomogeneities. Resonance nature of the transmission leads to the gain factor in scattering cross section of some orders of magnitude. This effect depends strongly on the total wave vector and becomes essential only for the very long-wave-length neutrons. Exploring the DWBA method, one may explain qualitative effects of the resonance shift and mode mixing observed with filters which feature relatively strong scattering. At the same time, using filters which feature only a weak scattering we did not observe any shift of the resonance within the limits of experimental error. Based on these results one may conclude that phenomena of the shift of the resonance position are caused at least mostly by the resonance scattering of neutrons during the tunneling.

Acknowledgements. Authors are very grateful to I. Anderson, E. Kats and V. Nosov for the fruitful discussions. This work was partly supported by the INTAS (grant 00-0043).

REFERENCES

1. *Seregin A. A.* // JETP. 1977. V. 73. P. 1634.
2. *Pokotilovskii Yu. N., Stoyka A. D., Shelkova I. G.* // Pribory i tekhnika eksperimenta. 1980, No. 1. P. 62 (in Russian).
3. *Steinhauser K.-A. et al.* // Phys. Rev. Lett. 1980. V. 44. P. 1306.
4. *Pokotilovskii Yu. N., Novopoltsev M. I.* JINR commun. P3-81-821. Dubna, 1981 (in Russian).
5. *Novopoltsev M. I., Pokotilovskii Yu. N., Shelkova I. G.* // Nucl. Instr. Meth. A. 1988. V. 264. P. 518–520.
6. *Steyerl A. et al.* // Z. Phys. B. 1981. V. 41. P. 283.
7. *Steyerl A. et al.* // Physica B. 1988. V. 151. P. 36.
8. *Nosov V. G., Frank A. I.* // Phys. At. Nucl. 1994. V. 57. P. 968.
9. *Frank A. I., Nosov V. G.* // Phys. Lett. A. 1994. V. 188. P. 120.

10. *Frank A. I., Nosov V. G.* // Phys. At. Nucl. 1995. V. 58. P. 461.

11. *Bondarenko I. V. et al.* // J. Phys. Soc. Jap. 1996. V. 65. Suppl. A. P. 29.

12. *Bondarenko I. V. et al.* // V Intern. Seminar on Interaction of Neutron with Nuclei (ISINN-5). Dubna, 1997. P. 418.

13. *Bondarenko I. V. et al.* // JETP Lett. 1998. V. 67. P. 786.

14. *Bondarenko I. V. et al.* // Phys. At. Nucl. 1999. V. 62. P. 721.

15. *Bondarenko I. V. et al.* // VII Intern. Seminar on Interaction of Neutrons with Nuclei (ISINN-7). Dubna, 1999. P. 148–157.

16. *Frank A. I. et al.* // Proc. SPIE. 1999. V. 3767. P. 360.

17. *Bondarenko I. V. et al.* // Nucl. Instr. Meth. A. 2000. V. 440. P. 591.

18. *Frank A. I. et al.* // VIII Intern. Seminar on Interaction of Neutrons with Nuclei (ISINN-8). Dunba, 2000. P. 448–453.

19. *Frank A. I. et al.* // Phys. Lett. A. 2003. V. 311. P. 6.

20. *Foldy L. I.* // Phys. Rev. 1945. V. 767. P. 107.

21. *Ignatovich V.* The Physics of Ultra-cold Neutrons. Oxford: Clarendon, S. a.

22. *Ignatovich V. K., Utsuro M.* // Phys. Rev. B. 1997. V. 755. P. 14774.

23. *Barabanov A. L., Belyaev S. T.* // Yad. Fiz. 1999. V. 762. P. 824.

24. *Nosov V. G., Frank A. I.* // Phys. Rev. A. 1997. V. 755. P. 1129.

25. *Frank I. M.* Neutron Optics and Ultracold Neutrons // Proc. of the II Intern. School on Neutron Physics. Dunba, 1974. P. 19–41; Usp. Fiz. Nauk. 1991. V. 161, No. 11. P. 110.

26. *Horn V. A. et al.* // Phys. Rev. A. 1983. V. 728. P. 1.

27. *Steyerl A. et al.* // Phys. Lett. A. 1986. V. 7116. P. 347.

28. *Sinha S. K. et al.* // Phys. Rev. B. 1988. V. 738. P. 2297.

29. *Holy V. et al.* // Phys. Rev. B. 1993. V. 747. P. 15896.

30. *Holy V., Baumbach T.* // Phys. Rev. B. 1994. V. 749. P. 10668.

31. *Toperverg B., Schaerpf O., Anderson I.* Preprint PNPI 2209. Gatchina, 1997; Physica B. 2000. V. 276–278. P. 954.

32. *Toperverg B.* // Appl. Phys. A. 2002. V. 74. P. S1560.

Received on December 29, 2004.

Редактор *Н. С. Скокова*

Подписано в печать 15.03.2005.
Формат $60 \times 90/16$. Бумага офсетная. Печать офсетная.
Усл. печ. л. 1,25. Уч.-изд. л. 1,8. Тираж 300 экз. Заказ № 54824.

Издательский отдел Объединенного института ядерных исследований
141980, г. Дубна, Московская обл., ул. Жолио-Кюри, 6.
E-mail: publish@pds.jinr.ru
www.jinr.ru/publish/